

**Transition metal embedded C₃N monolayers as promising catalysts for the
hydrogen evolution reaction**

Yameng Zhao^{1,2}, Dongwei Ma^{2,*}, Jing Zhang², Zhansheng Lu³,
and Yuanxu Wang^{1,*}

¹*Institute for Computational Materials Science, School of Physics and Electronics,
Henan University, Kaifeng 475004, China*

²*School of Physics, Anyang Normal University, Anyang 455000, China*

³*College of Physics and Materials Science, Henan Normal University, Xinxiang
453007, China*

Supporting Information

*Corresponding author. E-mail: dwmachina@126.com (Dongwei Ma).

*Corresponding author. E-mail: wangyx@henu.edu.cn (Yuanxu Wang).

Table S1. Zero-point energy (E_{ZPE} in eV) and entropy multiplied by T (T = 298.15 K and TS in eV) for the H atom adsorbed on the M and M-C1 sites for the M-CC catalysts.

Note that the value of E_{ZPE} is 0.31 eV for the H atom adsorbed on the C atom of the pristine C₃N monolayer.

Sites	E_{ZPE}	TS	Sites	E_{ZPE}	TS
Ti	0.15	0.03	Ti-C1	0.28	0.00
V	0.16	0.02	V-C1	0.26	0.00
Cr	0.15	0.03	Cr-C1	0.29	0.00
Mn	0.18	0.02	Mn-C1	0.30	0.00
Fe	0.19	0.01	Fe-C1	0.29	0.00
Co	0.19	0.02	Co-C1	0.29	0.00
Ni	0.16	0.03	Ni-C1	0.30	0.00
Cu	0.13	0.03	Cu-C1	0.30	0.00
Zn	0.16	0.02	Zn-C1	0.30	0.00
Mo	0.17	0.02	Mo-C1	---	---
Ru	0.18	0.02	Ru-C1	0.39	0.00
Rh	0.19	0.02	Rh-C1	0.30	0.00
Pd	0.17	0.03	Pd-C1	0.30	0.00
Ag	0.11	0.04	Ag-C1	0.30	0.00
Os	0.19	0.02	Os-C1	0.36	0.00
Ir	0.20	0.02	Ir-C1	0.30	0.00
Pt	0.18	0.03	Pt-C1	0.30	0.00
Au	0.13	0.03	Au-C1	0.31	0.00

Table S2. The formation energy (E_f in eV) for the various TM@C₃N systems and the binding energy (E_b in eV) for the M-CC systems.

	E_f		E_f		E_f		$E_f (E_b)$
Ti-C	2.81	Ti-N	4.04	Ti-CN	3.08	Ti-CC	1.00 (-3.39)
V-C	3.56	V-N	4.74	V-CN	3.81	V-CC	1.54 (-3.30)
Cr-C	3.58	Cr-N	4.00	Cr-CN	3.69	Cr-CC	1.28 (-3.55)
Mn-C	3.73	Mn-N	3.96	Mn-CN	2.78	Mn-CC	0.71 (-4.13)
Fe-C	3.64	Fe-N	3.78	Fe-CN	3.06	Fe-CC	1.10 (-3.74)
Co-C	3.89	Co-N	3.52	Co-CN	2.59	Co-CC	0.73 (-4.10)
Ni-C	4.08	Ni-N	4.43	Ni-CN	1.88	Ni-CC	0.49 (-4.34)
Cu-C	4.64	Cu-N	5.54	Cu-CN	2.81	Cu-CC	2.04 (-2.79)
Zn-C	3.69	Zn-N	4.81	Zn-CN	4.08	Zn-CC	2.08 (-2.76)
Mo-C	5.03	Mo-N	5.77	Mo-CN	4.81	Mo-CC	3.09 (-1.74)
Ru-C	4.48	Ru-N	4.48	Ru-CN	4.40	Ru-CC	2.77 (-2.06)
Rh-C	4.47	Rh-N	3.88	Rh-CN	3.51	Rh-CC	1.60 (-3.24)
Pd-C	4.94	Pd-N	5.32	Pd-CN	2.86	Pd-CC	1.38 (-3.49)
Ag-C	5.65	Ag-N	6.61	Ag-CN	4.22	Ag-CC	3.28 (-1.55)
Os-C	5.51	Os-N	5.50	Os-CN	4.57	Os-CC	3.15 (-1.69)
Ir-C	5.35	Ir-N	4.73	Ir-CN	3.46	Ir-CC	1.79 (-3.05)
Pt-C	5.20	Pt-N	5.54	Pt-CN	2.08	Pt-CC	0.90 (-3.93)
Au-C	5.82	Au-N	6.80	Au-CN	2.97	Au-CC	2.38 (-2.45)

Table S3. Net Bader charge (Q in e) of the doped TM atom and the C atom bonded to it for the M-CC systems. The positive charge value means the atom loses electrons.

	Q		Q		Q		Q
Ti	1.45	Ti-C1	0.14	Mo	1.21	Mo-C1	0.23
V	1.31	V-C1	0.19	Ru	0.74	Ru-C1	0.27
Cr	1.22	Cr-C1	0.21	Rh	0.54	Rh-C1	0.32
Mn	1.24	Mn-C1	0.21	Pd	0.55	Pd-C1	0.37
Fe	1.00	Fe-C1	0.22	Ag	0.75	Ag-C1	0.32
Co	0.75	Co-C1	0.28	Os	0.83	Os-C1	0.22
Ni	0.71	Ni-C1	0.32	Ir	0.63	Ir-C1	0.30
Cu	0.84	Cu-C1	0.29	Pt	0.56	Pt-C1	0.37
Zn	1.05	Zn-C1	0.28	Au	0.69	Au-C1	0.32

Table S4. Spin moment (M in μ_B) of the M-CC systems.

	M		M
Ti-CC	0.66	Mo-CC	0.93
V-CC	1.99	Ru-CC	0.00
Cr-CC	3.20	Rh-CC	0.00
Mn-CC	3.78	Pd-CC	0.00
Fe-CC	2.39	Ag-CC	0.00
Co-CC	0.80	Os-CC	0.00
Ni-CC	0.00	Ir-CC	0.00
Cu-CC	0.00	Pt-CC	0.00
Zn-CC	0.00	Au-CC	0.00

Table S5. ΔG_H (in eV) for the H atom on the M-C2, M-C3, M-C4, and M-C5 sites.

Sites	ΔG_H	Sites	ΔG_H	Sites	ΔG_H
Ti-C2	0.63	Ni-C2	0.52	Pd-C2	0.48
Ti-C3	1.35	Ni-C3	1.19	Pd-C3	1.14
Ti-C4	1.01	Ni-C4	1.09	Pd-C4	1.00
Ti-C5	1.14	Ni-C5	1.25	Pd-C5	1.26
V-C2	0.65	Cu-C2	0.71	Ag-C2	0.78
V-C3	1.23	Cu-C3	1.07	Ag-C3	1.13
V-C4	0.97	Cu-C4	1.07	Ag-C4	1.07
V-C5	1.27	Cu-C5	1.00	Ag-C5	1.08
Cr-C2	0.47	Zn-C2	0.50	Os-C2	0.20
Cr-C3	1.05	Zn-C3	0.87	Os-C3	0.94
Cr-C4	0.98	Zn-C4	0.92	Os-C4	0.79
Cr-C5	1.12	Zn-C5	1.06	Os-C5	1.21
Mn-C2	0.41	Mo-C2	0.58	Ir-C2	0.19
Mn-C3	1.15	Mo-C3	1.29	Ir-C3	1.00
Mn-C4	1.06	Mo-C4	0.87	Ir-C4	0.86
Mn-C5	1.16	Mo-C5	1.22	Ir-C5	1.20
Fe-C2	0.35	Ru-C2	0.29	Pt-C2	0.40
Fe-C3	1.15	Ru-C3	1.00	Pt-C3	1.17
Fe-C4	1.02	Ru-C4	0.80	Pt-C4	1.02
Fe-C5	1.18	Ru-C5	1.28	Pt-C5	1.23
Co-C2	0.35	Rh-C2	0.26	Au-C2	0.71
Co-C3	1.10	Rh-C3	1.00	Au-C3	1.16
Co-C4	0.98	Rh-C4	0.85	Au-C4	1.08
Co-C5	1.23	Rh-C5	1.24	Au-C5	1.09

Table S6. ΔG_H (in eV) for the second H atom adsorbed on the M-CC catalysts.

Sites	ΔG_H	Sites	ΔG_H	Sites	ΔG_H
Ti-C1	0.17	Ni-C1	0.17	Pd-C2	0.24
V-C1	0.22	Cu-C2	0.13	Ag-C2	-0.01
Cr-C2	0.20	Zn	0.18	Os-C1	-0.08
Mn-C2	0.14	Mo-C1	0.56	Ir-C1	0.35
Fe-C1	0.37	Ru-C1	0.14	Pt-C2	0.19
Co-C1	0.39	Rh-C1	0.26	Au-C2	0.00

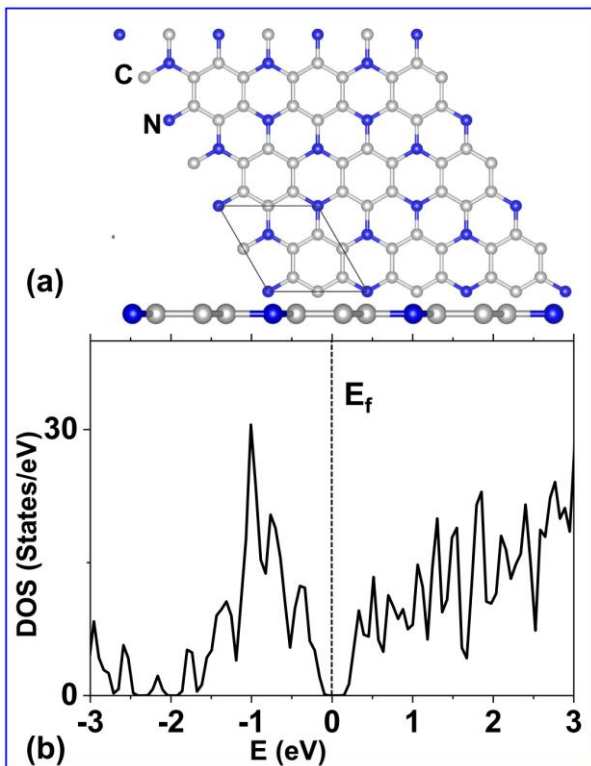


Fig. S1. (a) Top and side views of the (3×3) supercell of the pristine C₃N monolayer, of which the primitive cell is enclosed by the solid lines. (b) The TDOS of the C₃N monolayer shown in (a). The Fermi level (E_f) is set to 0 eV and indicated by the vertical dashed line.

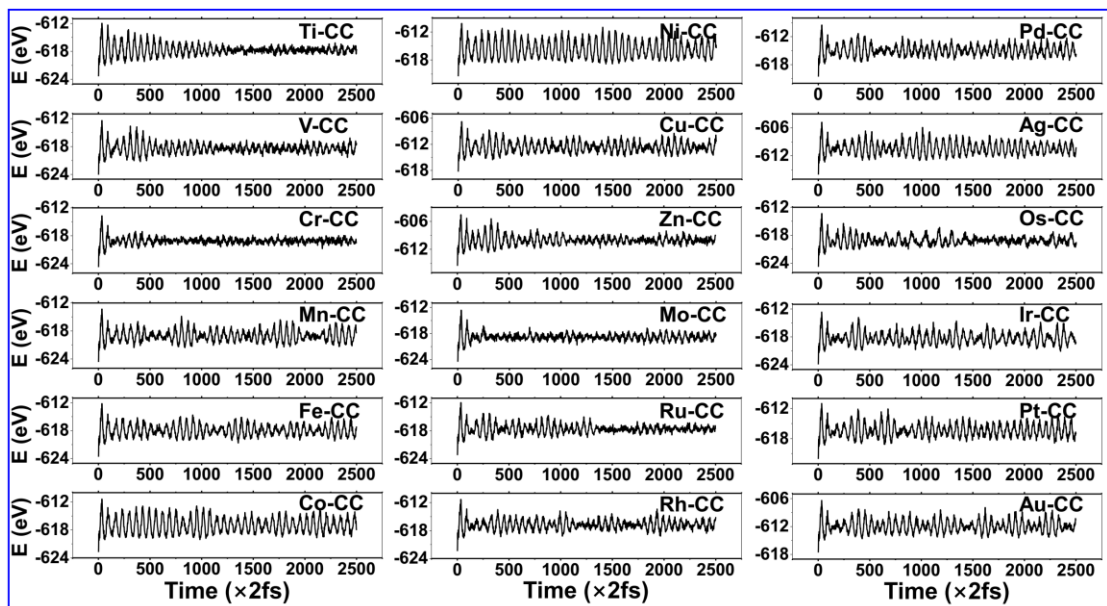


Fig. S2. Variation of the energy against the time for the AIMD simulation of the M-CC catalysts. The simulation has been run under 600 K for 5 ps with a time step of 2 fs.

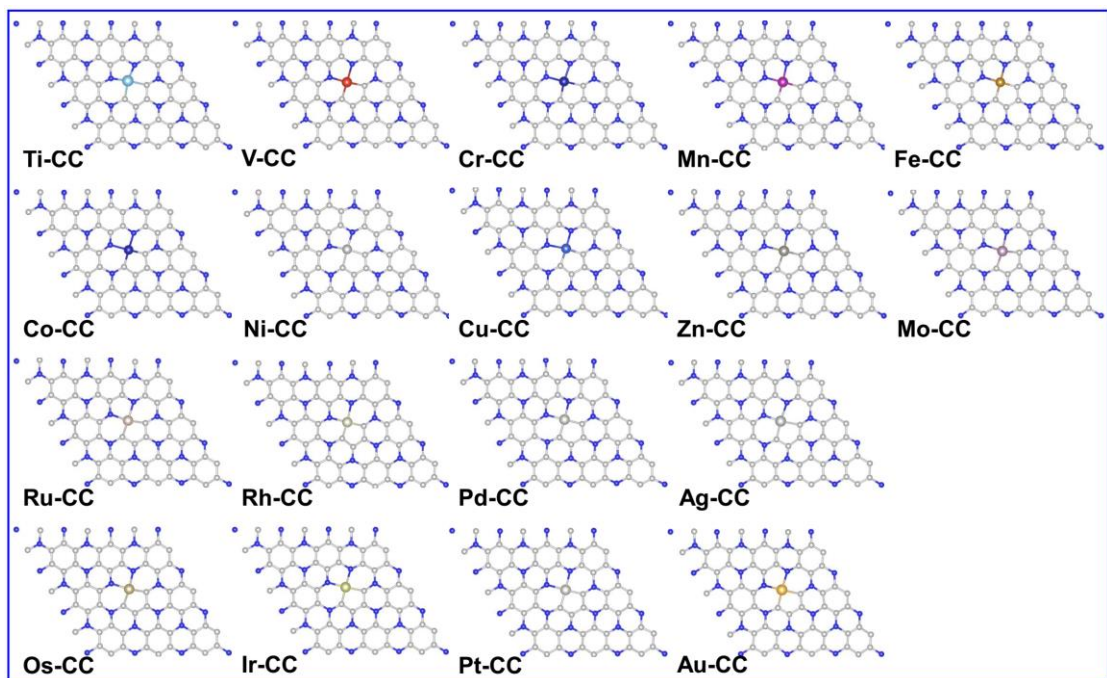


Fig. S3. The final structures of the M-CC catalysts after the AIMD simulation.

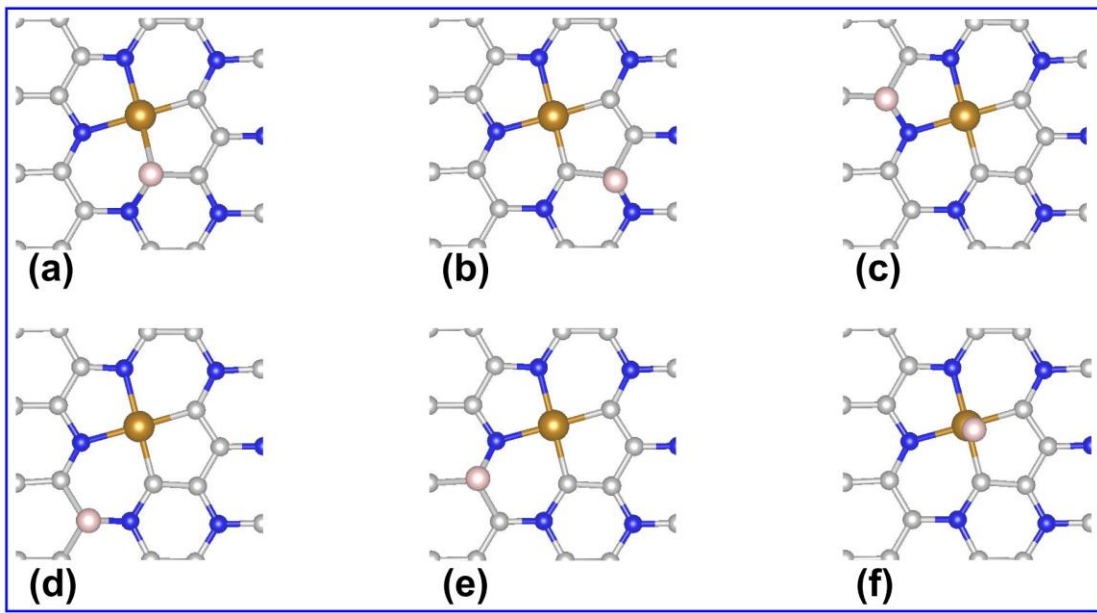


Fig. S4. Top views of the typical H adsorption configurations for the various sites of the M-CC catalyst, including M-C1 (a), M-C2 (b), M-C3 (c), M-C4 (d), M-C5 (e), and M (f).

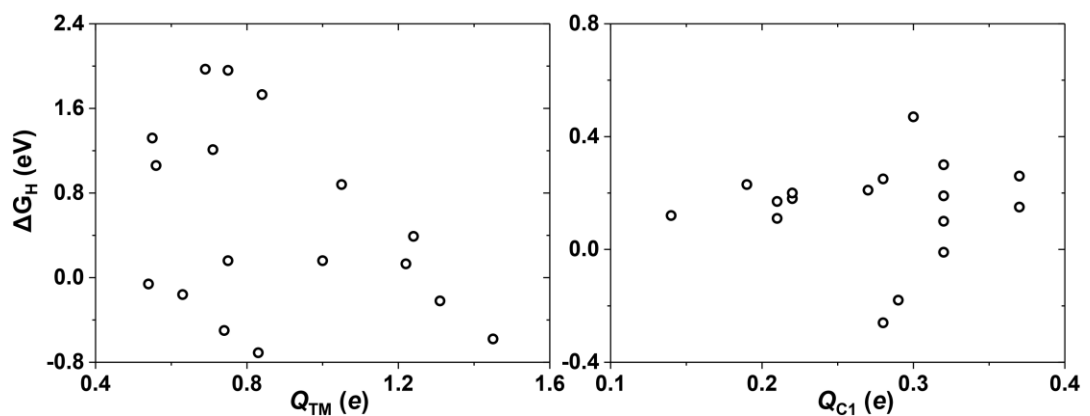


Fig. S5. Relationships between the calculated ΔG_H and the net charges on the embedded TM atoms (left panel) and the M-C1 atoms (right panel). Q_{TM} and Q_{C1} are the net charges on the embedded TM atoms and the M-C1 atoms, respectively.

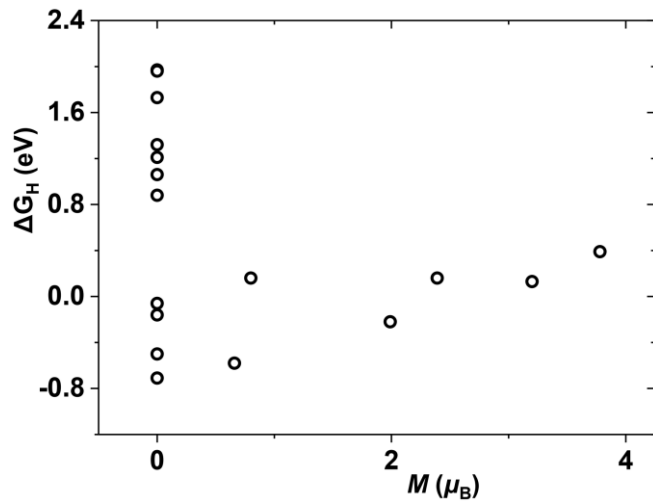


Fig. S6. Relationships between the calculated ΔG_H for the embedded TM atom sites and the spin magnetic moments.

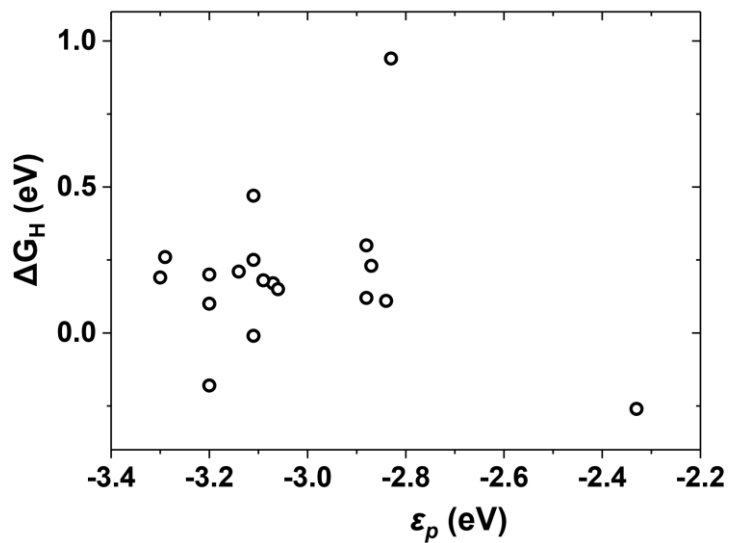


Fig. S7. Relationship between ΔG_H and ε_p for the C atom of the pristine C_3N monolayer and the M-C1 atoms. The integral domains is [-5 eV, 0 eV].

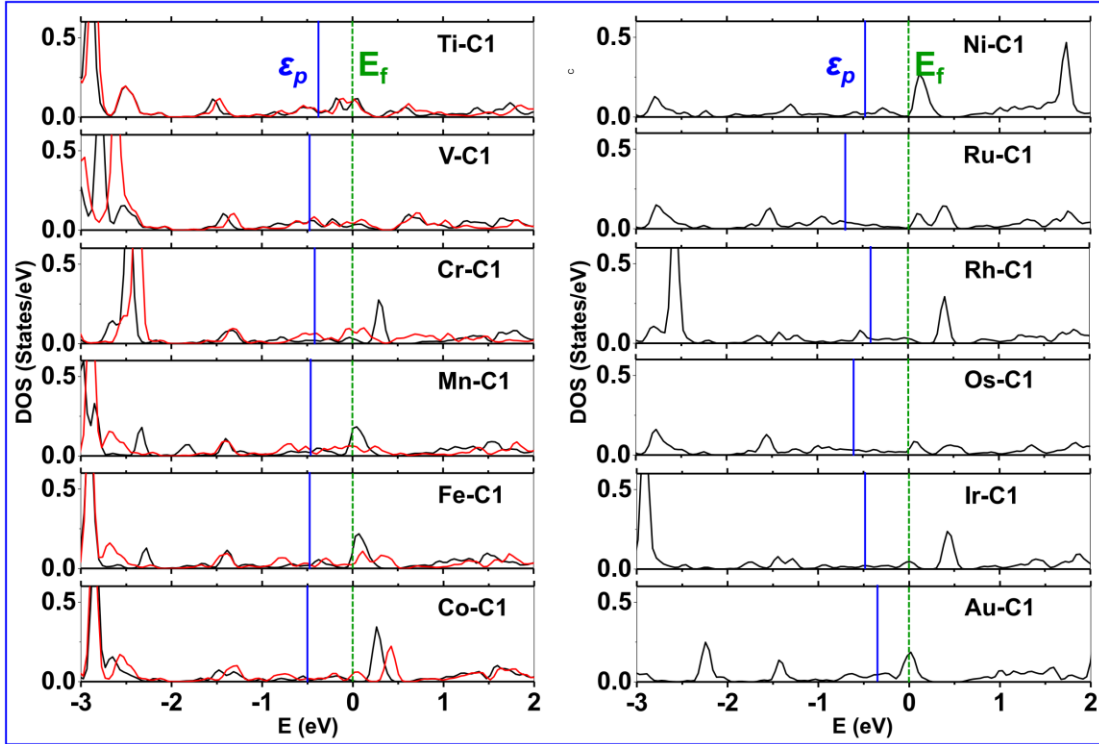


Fig. S8. The LDOS projected on the $2p$ orbitals of the M-C1 atoms for Ti, V, Cr, Mn, Fe, Co, Ni, Ru, Rh, Os, Ir, and Au-CC systems. The vertical blue line indicates the position of the p -band center (ε_p). In the left panel, the C atom has net spin magnetic moment, and the black and red curves denote the spin-up and spin-down states, respectively. For the nonmagnetic systems, only the spin-up part of the LDOS can be seen. The Fermi level (E_f) is set to 0 eV and indicated by the green dashed line.

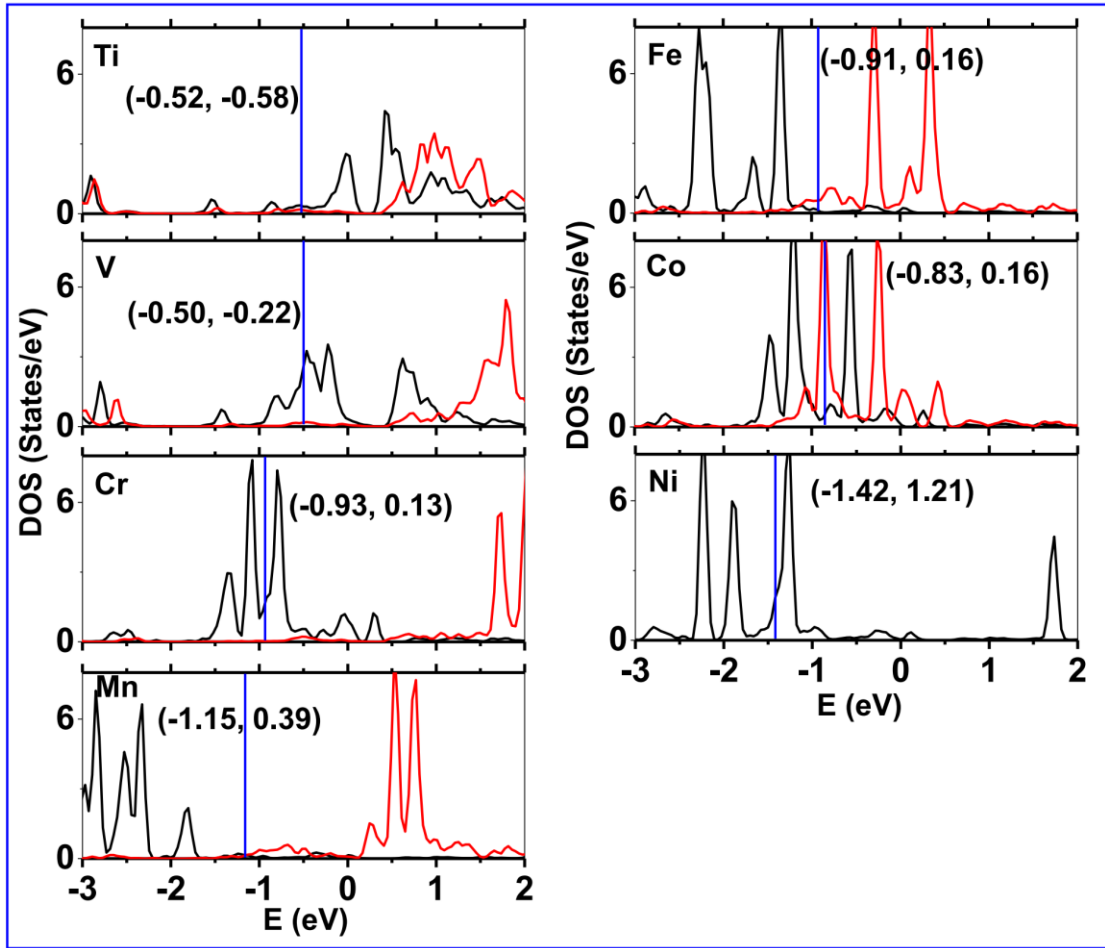


Fig. S9. The LDOS projected on the 3d orbitals of the doped TM atoms for Ti, V, Cr, Mn, Fe, Co, and Ni-CC. The vertical blue line indicates the position of the d -band center (ε_d). For the spin-polarized systems, and the black and red curves denote the spin-up and spin-down states, respectively. For the nonmagnetic systems, only the spin-up part of the LDOS can be seen. The Fermi level is set to 0 eV. The values of the calculated ε_d (former) and the relevant ΔG_H (latter) are given in the parenthesis.

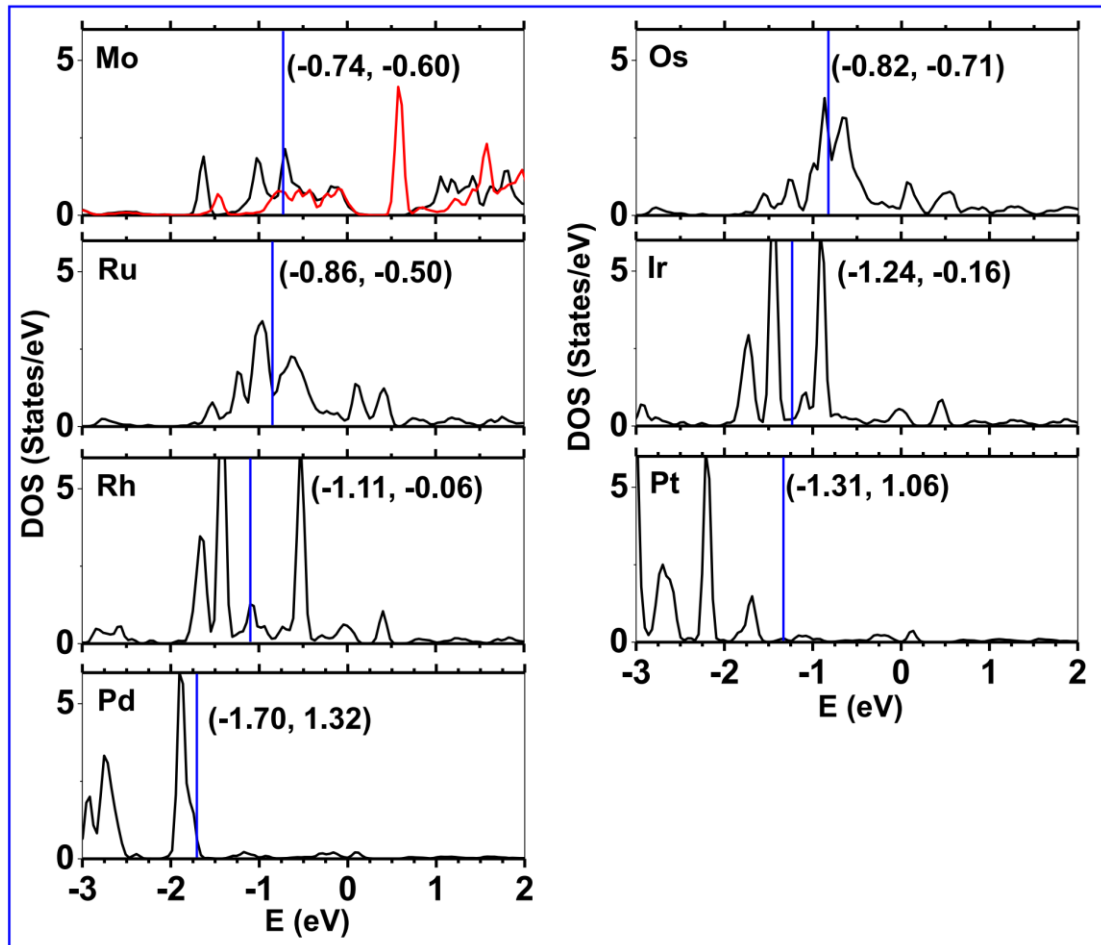


Fig. S10. Similar to Fig. S9, except that it is for the Mo, Ru, Rh, Pd, Os, Ir, and Pt-CC.

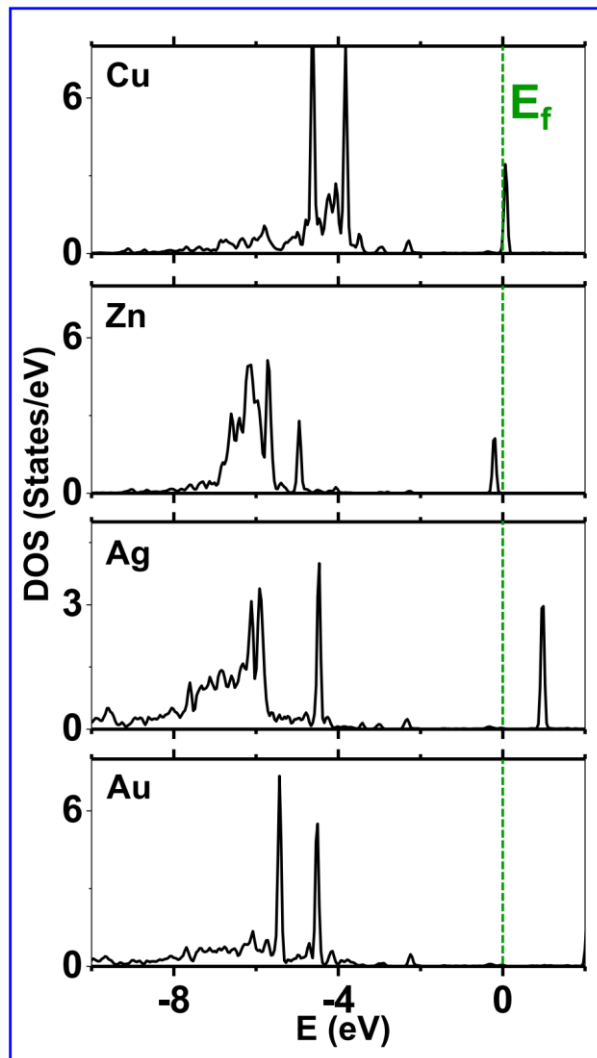


Fig. S11. The LDOS projected on the d orbitals of the doped TM atoms for Cu, Zn, Ag, and Au-CC systems. The Fermi level is set to 0 eV and indicated by the green dashed line. Due to that these systems are nonmagnetic, the spin-up part of the LDOS is overlapped with the spin-down part.

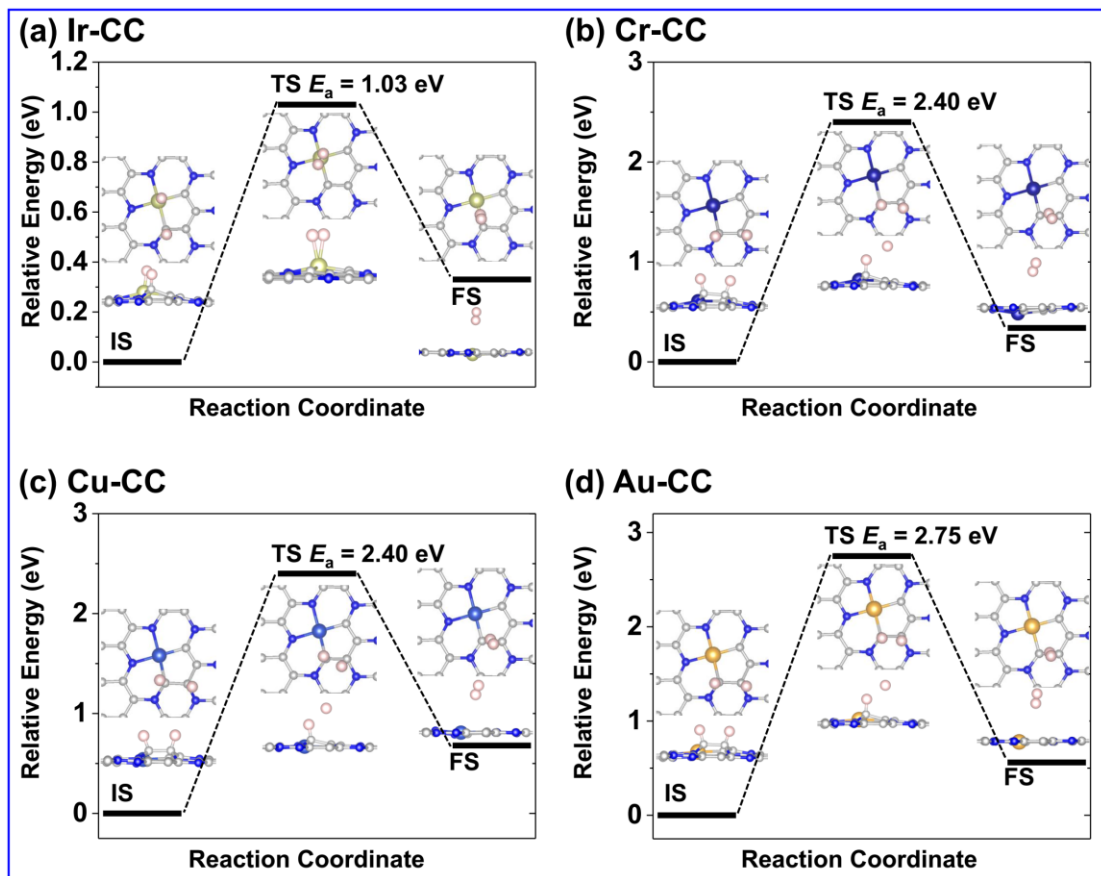


Fig. S12. Minimum-energy pathways of the HER under the Tafel mechanism for the Ir-CC (a), Cr-CC (b), Cu-CC (c), and Au-CC (d) catalysts. The insets are the corresponding atomic structures of the IS, TS, and FS. The kinetic barriers (E_a in eV) are given.